
PERGAMON

Journal of Quantitative Spectroscopy & Radiative Transfer 74 (2002) 697–718

Journal of Quantitative Spectroscopy & Radiative Transfer

www.elsevier.com/locate/jqsrt

Numerical investigation of the effect of soot aggregation on the radiative properties in the infrared region and radiative heat transfer

V. Eymet[a], A.M. Brasil[b], M. El Hafi[a], T.L. Farias[c,*], P.J. Coelho[c]

[a] *Centre Energétique-Environnement, Ecole des Mines d'Albi, Campus Jarlard, Route de Teillet 81000 Albi, France*
[b] *Mechanical Engineering Department, Universidade Federal de Pernambuco, Rua Acadêmico Hélio Ramos, Cidade Universitária, 50.740-530 Recife-PE, Brazil*
[c] *Mechanical Engineering Department, Instituto Superior Técnico, Universidade Tecnica de Lisboa, Av Rovisco Pais, 1049-001 Lisboa, Portugal*

Received 13 September 2001; accepted 29 November 2001

Abstract

The effect of aggregation on soot radiative properties in the infrared region of the spectrum is numerically investigated using Rayleigh–Debye–Gans theory for fractal aggregates (RDG-FA). In order to use the RDG-FA theory for a wide range of aggregate sizes and wavelengths, the predicted phase functions, scattering and absorption coefficients are compared with a more accurate theory, the integral equation formulation for scattering—IEFS. The importance of scattering when compared with absorption is investigated, as well as the effect of aggregation on the phase function shape and on the scattering cross section. It is concluded that in the case of small aggregates formed with small primary particles the scattering coefficient is negligible compared with the absorption coefficient, and scattering and aggregation of primary particles can be ignored. Thus, the Rayleigh approximation can be used leading to isotropic scattering. In the case of large aggregates constituted by large primary particles, aggregation becomes important and the scattering cross section is of the same order of magnitude of the absorption cross section. Moreover, the phase function becomes highly peaked in the forward direction. Therefore, the Rayleigh and the equivalent volume Mie sphere approximations are not valid, and the RDG-FA method emerges as a good compromise between accuracy and simplicity of application. However, radiative transfer calculations between two infinite, parallel, black walls show that scattering may always be neglected in the calculation of total radiative heat source and heat fluxes to the walls. The minor influence of scattering on the accuracy of the predictions is explained by the shift between the spectral region where scattering is important and the region where the spectral radiative heat source is large.

Keywords: Soot; Scattering; Fractal aggregates; Rayleigh–Debye–Gans/fractal aggregate (RDG-FA) theory; Integral equation formulation for scattering (IEFS)

* Corresponding author. Tel.: +351-21-841-7929; fax: +351-21-847-5545.
E-mail address: fariastl@navier.ist.utl.pt (T.L. Farias).

0022-4073/02/$ - see front matter
PII: S0022-4073(01)00280-1

1. Introduction

Radiative heat transfer in absorbing, emitting, and scattering media at high temperatures is of particular interest in many engineering technologies, including internal combustion engines, gas turbines, industrial furnaces, fire safety, and atmospheric radiation [1,2]. It is well known that the presence of soot in combustion systems enhances heat transfer rates significantly due to the continuum radiation in the infrared regions of the wavelength spectrum. Radiation predictions require the knowledge of a wide variety of properties such as soot concentration and temperature distributions in such particulate-laden media. In addition, information about the spectral radiative properties of soot, such as phase function and scattering coefficient is also required. These properties are characterized in terms of the refractive index, size and morphology [3].

Earliest literature on soot radiation in flames generally considered soot shape as spherical, so that simple predictions based on the Rayleigh theory for the nanosize primary particles, or the Mie theory with a volume-equivalent diameter were possible. Unfortunately, ultrafine particles (including soot) produced in combustion systems form aggregates with a wide range of sizes and shapes [4,5]. As a result of this complex morphology, Charalampopoulos and Chang [6], and Ku and Shim [7] investigated the effect of soot morphology on flame radiation by considering aggregates of small primary particles having relatively low number of primary particles (<32). Radiative properties of fractal soot aggregates have recently received considerable attention [8–11]. However, these investigations, as well as those reported in [12,13], were generally limited to fundamental optical cross sections at visible wavelengths because of their specific interest in developing tools for laser diagnostics in particulate-laden media. Farias et al. [13] investigated the effect of aggregation on the soot phase function, scattering albedo and flame emissivity. However, no simple solution concerning the prediction of phase functions and scattering cross sections of soot, such as via Rayleigh–Debye–Gans theory for fractal aggregates (RDG-FA), was proposed which would considerably help researchers to model the radiative heat transfer in combustion enclosures where soot is present. In addition, that study focused on the near infrared and visible wavelengths and for aggregates containing up to 256 primary particles. Furthermore, it is well known that the Rayleigh theory may be used to calculate the absorption coefficient for all but the largest soot primary particles, while scattering may be neglected. However, it is still not clear whether scattering may be neglected or not for the large soot agglomerates found in combustion systems.

Based on the previous considerations, the main objective of the present study is to quantitatively analyze the effect of soot aggregation on the scattering coefficient and phase function in the infrared region, and to investigate whether scattering may be neglected or not in the calculation of radiative heat transfer in enclosures with high soot concentration and very large soot agglomerates. Moreover, it is our purpose to verify if simple expressions based on the RDG-FA theory can be used to characterize the phase function of aggregated soot particles, in order to easily model radiative heat transfer in a sooting environment. To evaluate the RDG-FA theory in the infrared region, a more accurate theory was used. This theory, referred to as integral equation formulation for scattering (IEFS), accounts for multiple scattering and self-interactions among small spherical particles [9,14].

The different light scattering theories addressed and the numerical method adopted to simulate the aggregates are presented in Section 2. The evaluation of IEFS and RDG-FA theories in the infrared region is presented in Section 3. Then, an investigation of the effect of aggregation on the scattering properties of soot is presented and the influence of aggregation is quantified. The influence of soot

aggregation on radiative fluxes and radiative heat sources is investigated in Section 5. The main conclusions of the present study are summarized in the last section.

2. Theoretical methods

2.1. Radiative transfer equation

The radiative transfer equation (RTE) is a mathematical statement of the conservation principle applied to a monochromatic pencil (bundle) of radiation traveling along a path through a medium. Radiation traveling along a path is attenuated by absorption and out-scattering, and is enhanced by emission and in-scattered radiation from other directions. All these effects are accounted for in the RTE [3,15] that can be expressed as

$$\mathbf{s}\cdot\nabla I_\lambda(\mathbf{r},\mathbf{s}) = -K_\lambda I_\lambda(\mathbf{r},\mathbf{s}) + K_{a\lambda} I_{b\lambda}(\mathbf{r}) + \frac{K_{s\lambda}}{4\pi}\int_{4\pi} I_\lambda(\mathbf{r},\mathbf{s}')\Phi(\mathbf{s}',\mathbf{s})\,\mathrm{d}\Omega', \tag{1}$$

where $I_\lambda(\mathbf{r},\mathbf{s})$ is the spectral radiation intensity at position $\mathbf{r}$ along a path with unit vector $\mathbf{s}$, $I_{b\lambda}$ is the spectral blackbody radiation intensity, $\Phi(\mathbf{s}',\mathbf{s})$ is the scattering phase function, which describes the probability that a ray from direction $\mathbf{s}'$ is scattered into direction $\mathbf{s}$, and $K_{a\lambda}$, $K_{s\lambda}$ and $K_\lambda = K_{a\lambda} + K_{s\lambda}$ are the spectral absorption, scattering and extinction coefficients of the medium, respectively.

The boundary condition for a diffusely emitting and reflecting opaque wall at a point $\mathbf{r}_w$ on the surface is given by

$$I_\lambda(\mathbf{r}_w,\mathbf{s}) = \varepsilon_\lambda I_{b\lambda}(\mathbf{r}_w) + \frac{\rho_\lambda}{\pi}\int_{\mathbf{n}\cdot\mathbf{s}'<0} I_\lambda(\mathbf{r}_w,\mathbf{s}')|\mathbf{n}\cdot\mathbf{s}'|\,\mathrm{d}\Omega', \tag{2}$$

where $\mathbf{n}$ is the local unit outward normal vector, and ε_λ and ρ_λ are the spectral emissivity and reflectivity of the surface, respectively. Here $\mathbf{s}$ is the direction of the outgoing radiation intensity and $\mathbf{s}'$ is the incoming direction associated with the elementary solid angle $\mathrm{d}\Omega'$.

Two major difficulties may be identified in the analysis of the RTE. First, the RTE is an integro-differential equation and an exact solution may only be obtained for a very limited set of problems. Hence, a numerical method is generally required to solve the RTE. The second problem deals with the evaluation of the scattering and absorption coefficients, as well as the phase function, which depend on wavelength, media composition, temperature, pressure, type of particles, particle concentration, etc. The present paper addresses the second problem for the particular case of soot particles.

2.2. Radiative predictions for aggregated spherical particles

The RDG-FA and the IEFS theories were employed in this study to calculate phase functions, scattering and absorption cross sections of soot aggregates. These two scattering theories are briefly described in the following sections.

2.2.1. The Rayleigh–Debye–Gans theory for fractal aggregates

The RDG-FA scattering theory is based on methods described in [16–19]. Present considerations, however, will be limited to the extended version due to Köylü and Faeth [12], which allows for the

presence of the power-law regime when finding total scattering cross sections, because this regime is important for large aggregates. The major assumptions of this approach with respect to soot aggregate physical properties are as follows: spherical primary particles have constant diameters, primary particles have uniform refractive indices, primary particles just touch one another, and the aggregates are mass-fractal objects. The justification of these assumptions for soot aggregates is discussed in [12,20].

The mass fractal approximation for aggregates of constant-diameter spherical primary particles implies the following relationship between the number of primary particles in an aggregate, N, and the radius of gyration of the aggregate, R_g [17]:

$$N = k_g(2R_g/d_p)^{D_f}, \tag{3}$$

where d_p is the diameter of a soot primary particle. The fractal dimension, D_f, and the pre-factor, k_g, in Eq. (3) appear to be relatively universal properties of soot aggregates, as described later on. Thus, Eq. (3) provides a critical relationship between N, a quantity that is readily measured, and R_g, an important parameter required by the RDG scattering theory.

In addition to the RDG approximation, it is also assumed that the primary particles are small enough to satisfy the Rayleigh scattering approximation as individual particles, and multiple scattering is neglected. In other words, the light scattered in the far field domain is composed of a vector summation of the scattering light of each primary particle. Assuming that the individual particles act like Rayleigh scatterers is reasonable because primary particle optical size parameters, x_p, are generally lower than 0.1 for soot in the infrared wavelength ranges. This implies that the total scattering and absorption cross sections of individual primary particles are within 1% and 5%, respectively, of estimates based on the Rayleigh scattering approximation for typical refractive indices for soot [20]. This yields the following expressions for the absorption, C_a^p, and scattering, C_s^p, cross sections of individual primary particles [21,22]:

$$C_a^p = \frac{4\pi x_p^3}{k^2}\,\mathrm{Im}\left(\frac{m^2-1}{m^2+2}\right), \tag{4a}$$

$$C_s^p = \frac{8\pi x_p^6}{3k^2}\left|\frac{m^2-1}{m^2+2}\right|^2, \tag{4b}$$

where $m = \eta + i\kappa$ is the complex refractive index of soot, k is the wave number and Im denotes the imaginary party of a complex number. According to the RDG approximation, differential scattering cross sections for aggregates of a given size (after averaging over all orientations of each aggregate within a statistically-significant monodisperse aggregate population) satisfy the following formulas [22]:

$$C_{vv}^a(\Theta) = C_{hh}^a(\Theta)/\cos^2(\Theta) = N^2 C_{vv}^p f(qR_g), \tag{5}$$

where C^a and C^p denote cross sections of an agglomerate and a primary particle, respectively, the double subscripts identify the direction of polarization of the incident and scattered light (vv: vertical–vertical; hh: horizontal–horizontal), respectively, Θ is the scattering angle and q is the modulus of the scattering vector. The form factor, $f(qR_g)$, is expressed as follows in the Guinier and power-law

regimes [16–18]:

$$f(qR_g) = \exp(-q^2R_g^2/3) \quad \text{Guinier regime (where } q^2R_g^2 \leqslant 1.5D_f\text{)}, \tag{5a}$$

$$f(qR_g) = (qR_g)^{-D_f} \quad \text{power-law regime (where } q^2R_g^2 > 1.5D_f\text{)}. \tag{5b}$$

Here, the boundary between the Guinier and power-law regimes has been chosen according to Dobbins and Megaridis [19] to match the value and the derivative of $f(qR_g)$ where the two regimes meet. The total scattering cross section is given by

$$C_s^a = N^2 C_s^p g(k, R_g, D_f), \tag{6}$$

where the function $g(k, R_g, D_f)$ is given in [12]. It is also assumed that absorption is not affected by aggregation, while the extinction cross section is the sum of the absorption and scattering cross sections by definition, i.e.,

$$C_a^a = NC_a^p, \tag{7}$$

$$C_e^a = C_a^a + C_s^a. \tag{8}$$

The phase function is given by the following equation:

$$\Phi^a(\Theta) = \frac{4\pi}{C_s^a} \frac{C_{vv}^a(\Theta) + C_{hh}^a(\Theta)}{2}. \tag{9}$$

2.2.2. The integral equation formulation for scattering (IEFS)

The IEFS theory [9,13,14] divides an aggregate into sufficiently small units (the primary particles) so that the internal field within each particle is assumed to be uniform, and includes multiple scattering effects, self-interaction contributions, and satisfies energy conservation. The assumption of uniform electric field within a primary particle does not hold for touching spheres with large values of $|m-1|$, regardless of the smallness of x_p, and it has been shown that the contact point between the primary particles substantially increases the scattering and absorption properties of an aggregate [23]. However, soot aggregates, like any other type of combustion generated aggregates, are not constituted by single point touching particles. A certain degree of penetration of the neighboring primary particles, generally referred to as partial sintering, is present. This effect eliminates the single point contact area that is primarily responsible for the substantial increase of scattering and absorption properties. In the IEFS theory, the internal electrical field of each particle, $\boldsymbol{E}_j$, is obtained from the following system of $3N \times 3N$ linear equations:

$$\boldsymbol{E}_j = \left(\frac{3}{m^2+2}\right)\boldsymbol{E}_{\text{inc},j} + i\left(\frac{m^2-1}{m^2+2}\right)x_p^2 j_1(x_p)\sum_{l=1,l\neq j}^{N}\bar{\boldsymbol{T}}_{jl}\boldsymbol{E}_l + s_j\boldsymbol{E}_j; \quad j = 1,2,\ldots,N, \tag{10}$$

where $\boldsymbol{E}_{\text{inc}} = E_o \exp(ikz)$ represents the incident electric field propagating along the z-axis with a wave number of $k = 2\pi/\lambda$, $j_1(x_p)$ is the first-order spherical Bessel function of the first kind, s_j is the coefficient for self interaction and $\bar{\boldsymbol{T}}$ is the scattering matrix. Once the internal field of each spherical particle is known from Eq. (10), various optical cross sections can be obtained for an aggregate

with N uniform size particles (see, e.g., [13]). The differential scattering cross sections are given by

$$C_{\mathrm{pp}}^{\mathrm{a}}(\theta,\phi)=\frac{1}{k^2}x_{\mathrm{p}}^4 j_1^2(x_{\mathrm{p}})|m^2-1|^2\left|\sum_{j=1}^{N}\exp(-ikr_j\cos\beta_j)(E_{j,\theta}\hat{\theta}+E_{j,\phi}\hat{\phi})_{\mathrm{pp}}\right|^2. \tag{11}$$

In this equation the direction of the scattered field is represented using spherical coordinates, and θ and ϕ stand for the polar and azimuthal angles (unit vectors denoted by $\hat{\theta}$ and $\hat{\phi}$). The position of each individual particle is defined by the coordinates (r_j,θ_j,ϕ_j). The direction of polarization is denoted by subscript pp, which may stand for vv, vh, hv or hh, and $\cos\beta_j=\cos\theta_j\cos\theta+\sin\theta_j\sin\theta\cos(\phi_j-\phi)$.

The total scattering and absorption cross sections are given by

$$C_{\mathrm{s}}^{\mathrm{a}}=\frac{4\pi}{3k^2}x_{\mathrm{p}}^4 j_1^2(x_{\mathrm{p}})|m^2-1|^2\sum_{j=1}^{N}\sum_{k=1}^{N}\boldsymbol{E}_j\,\mathrm{Re}(\bar{\boldsymbol{T}}_{jk})\boldsymbol{E}_k^*, \tag{12a}$$

$$C_{\mathrm{a}}^{\mathrm{a}}=\frac{4\pi}{k^2}x_{\mathrm{p}}^2 j_1(x_{\mathrm{p}})\,\mathrm{Im}(m^2-1)\sum_{j=1}^{N}|\boldsymbol{E}_j|^2, \tag{12b}$$

where the superscript * represents the complex conjugate, and Re and Im denote the real and imaginary parts of a complex number, respectively. The phase function may be determined from Eq. (9).

This formulation satisfies the optical theorem, i.e., the sum of the total scattering and absorption cross sections is exactly equal to the extinction cross section of an aggregate [14,21]. Unfortunately, the IEFS method is computationally intensive for treating relatively large and/or polydisperse soot aggregates, because it requires the knowledge of the spatial position of the primary particles, as well as a large population of aggregates to obtain statistically significant results.

2.3. Numerical simulation of fractal-like aggregates

To compute the radiative properties using the IEFS theory it is necessary to know the primary particle positions within each aggregate. It has been shown that soot aggregates follow a mass fractal-like morphology that can be represented by Eq. (3). In this work, aggregates were numerically generated using a practical sequential algorithm that models the statistical fractal relationship given by that equation, rather than using the formal diffusion-limited cluster–cluster simulations [8,9,24,25]. Briefly, the aggregation process is initiated by randomly attaching individual and pairs of particles to each other. Once the position of every primary particle is known, the radius of gyration of the new aggregate is calculated from its definition, and it is checked if the fractal relationship given by Eq. (3) is satisfied. This procedure continues in order to form progressively larger clusters. Thirty-two different realizations of the same aggregate size, each sampled at 16 different orientations, were averaged to obtain statistically significant IEFS predictions with $<10\%$ numerical uncertainty (95% confidence interval).

2.4. Soot fractal properties

In spite of the complex appearance, various size and shape soot aggregates have been found to have a universal morphology with $D_f \cong 1.6$–1.9. On the contrary, the selection of universal values for the fractal pre-factor for cluster–cluster aggregates has been a controversial issue. Wu and Friedlander [26], and more recently Köylü et al. [27], have unified most of experimental and numerical data reported on this property. For example, the results published in the literature for k_g in cluster–cluster aggregates indicate values between 1.23 [28] and 3.47 [29]. The range of published results varies by $> 200\%$, clearly showing that this issue deserves further attention. In spite of the range of values published, it was found that the results based on numerically simulated aggregates are systematically lower than the values inferred from experimental data. Oh and Sorensen [30] have investigated the effect of overlapping between primary particles on the fractal properties and concluded that the fractal dimension, and particularly the fractal pre-factor, may vary considerably with the degree of overlapping. However, no final conclusion regarding the discrepancies between experimental results and numerical findings was drawn. Brasil et al. [25] found that the large discrepancies between the values reported for k_g appear to be related to the partial overlapping of primary particles, which leads to an increase of k_g while keeping the fractal dimension approximately constant. Therefore, it can be concluded that aggregates without overlapping should be simulated having lower values of k_g, while k_g will increase as overlapping increases, as systematically observed by several authors.

More recently, Brasil et al. [25] combined numerical predictions of light scattering with morphological fractal concepts based on Eq. (3) to estimate the fractal dimensions of cluster–cluster simulated aggregates. Their best estimates were $k_g = 1.3$ and $D_f = 1.8$. These results are in very good agreement with the great majority of the values presented by other authors for simulated aggregates (see [25] and references cited therein). Based on the previous considerations, aggregates used throughout the present work were simulated in such a manner to have $k_g \cong 1.3$ and $D_f \cong 1.8$.

3. Evaluation of the light scattering theories

3.1. Preliminary considerations

One of the main goals of the present work is to use the RDG-FA theory to investigate the effect of aggregation on the radiative properties. However, the RDG-FA theory neglects multiple scattering and, therefore, it is necessary to investigate its accuracy within the range of refractive indices typically exhibited by soot in the infrared region. This issue was addressed by comparing the results of RDG-FA with predictions from the more accurate IEFS theory within a wide range of x_p, N and m. The applicability of IEFS within this range was confirmed by using a compact aggregate with a spherical shape and comparing IEFS predictions with Mie results for an optically equivalent sphere. Based on these considerations, the applicability of IEFS is investigated first, and then the RDG-FA theory is evaluated by comparing its predictions with the results obtained from the IEFS theory.

A wide range of primary particle sizes and number of primary particles per aggregate was covered, namely, x_p in the range 0.01–0.1 and N between 1 (a single Rayleigh scatterer) and 256. Primary particles in soot aggregates usually have diameters < 60 nm, which combined with wavelengths

within the infrared region (1–10 μm) indicates that primary particle size parameters fall within the defined range. Concerning the refractive index, typical values that characterize soot particles in the infrared range were considered, namely $|m-1|=1$ to 4, and the following relationship between the real and imaginary parts of the refractive index was assumed: $n=k+1$. This assumption drastically simplifies the presentation of the results and closely follows the available data for the complex refractive index of soot in the infrared spectrum [3].

3.2. Evaluation of IEFS theory

The IEFS theory was checked by computing the scattering properties of sphere-like aggregates, and by comparing the results with Mie scattering predictions for optically equivalent sphere-like aggregates. In order to apply Mie scattering predictions to clusters involving N spherical primary particles with a spherical outer boundary, the following Maxwell–Garnett relationship was used:

$$\frac{(m_{\mathrm{e}}^2-1)}{(m_{\mathrm{e}}^2+2)}=f_{\mathrm{f}}\frac{(m^2-1)}{(m^2+2)}. \tag{13}$$

This equation has been used by several investigators (see, e.g., [31]) to find the effective refractive index of an equivalent sphere, m_{e}, as a function of the filling factor, f_{f}, defined as the ratio of the volume of the computational cell ($\pi d_{\mathrm{p}}^3/6$ for spherical cells) to the volume of bulk material.

The analysis was carried out using a sphere-like aggregate, similar to the arrangement employed in [31,32], formed by 136 spherical primary particles in a cubical lattice with a spherical outer boundary. The choice of a compact cluster for evaluating the performance of IEFS theory is quite conservative, because it represents the limiting case of a compact aggregate with fractal dimension, D_{f}, approaching three. In such an aggregate, effects of multiple scattering between primary particles are more intense than for practical fractal-like aggregates, such as soot, that exhibit more open-structure morphologies with $D_{\mathrm{f}}<2$. Optical cross sections, including absorption, total scattering cross sections and phase function were computed for the sphere-like cluster after averaging the calculations over 12 different orientations. This was necessary to reduce the effect of the staggered shape of the sphere-like cluster, which can affect the large angle scattering regimes.

The good accuracy of the IEFS theory for the different radiative properties can be seen in Figs. 1–3, which show the contours of the relative error of this theory, taking as exact the Mie equivalent sphere results. In fact, the errors of the absorption and scattering cross sections never exceed 6%, while the errors of the phase function are always $<2.5\%$, indicating that the IEFS formulation is suitable to estimate the radiative properties.

3.3. Evaluation of RDG-FA theory

Fig. 4 shows the percent deviation contours of the RDG-FA predictions from the IEFS results for the absorption cross section of soot aggregates. The percent deviation is defined as the ratio of the modulus of the difference between the values calculated by the two theories to the value computed using the IEFS theory, multiplied by 100. The results show that the RDG-FA approximation is best for small values of $|m-1|$ and x_{p}, as a consequence of the fundamental assumptions involved in its derivation. Similar observations were reported for spheres and cylinders by several investigators, as summarized in [22]. However, the requirements for the applicability of the RDG-FA theory are not

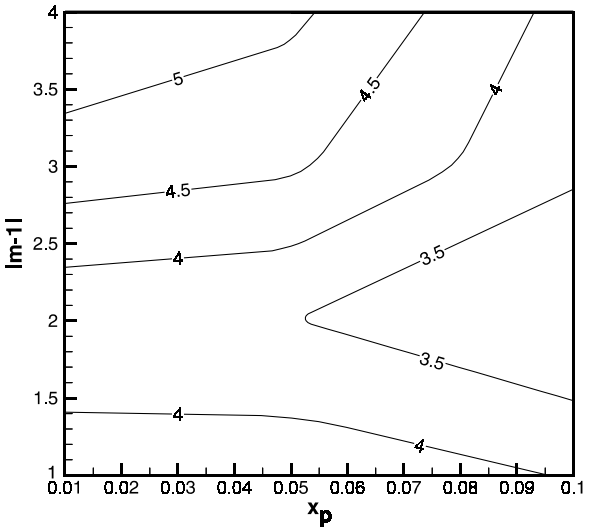

Fig. 1. Contours of the relative error of the absorption cross section calculated using the IEFS theory.

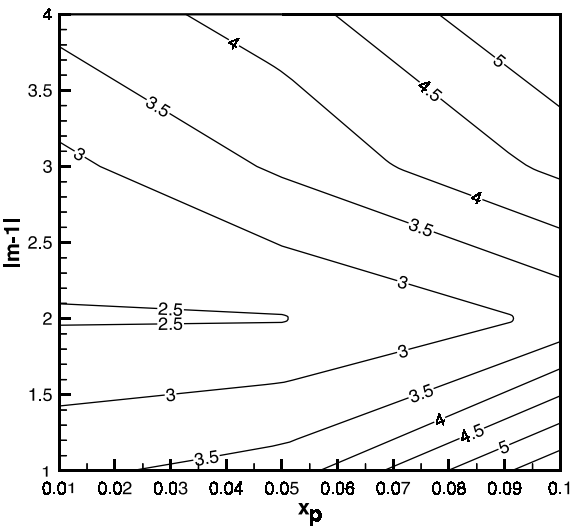

Fig. 2. Contours of the relative error of the scattering cross section calculated using the IEFS theory.

as strict as might be expected, because percent deviations $< 35\%$ are found over almost the whole range of parameters under investigation. From a physical point of view, low percent deviations are found whenever the absorption cross sections of an aggregate and the individual particles composing them act similarly, i.e., Eq. (7) is satisfied. The RDG-FA predictions deviate more from the IEFS results as N increases. Nevertheless, the RDG-FA theory seems to be fairly reliable throughout most of the domain considered, except in the regions where large x_p and $|m-1|$ are combined.

The percent deviation contours of the RDG-FA predictions from the IEFS results for the total scattering cross sections of aggregates are plotted in Fig. 5. The results exhibit trends similar to those reported for the absorption cross section. They confirm that the refractive index of particles does not have to be much smaller than 1, which is one of the classical requirements for the validity of the RDG theory [22]. In fact, the results suggest that the RDG-FA predictions are in fair agreement with the IEFS predictions for $|m-1| > 2$ as long as N and x_p are small.

Similar percent deviation contours for the phase function at scattering angles of 0° and 90° are illustrated in Fig. 6. Calculations were also performed for a scattering angle of 180°, but the results are not shown, since the order of magnitude of the deviation between the two theories is about the same found for $\Theta = 90^\circ$. Low percent deviations are associated to the range of $|m-1|$ and x_p values for which multiple scattering and self-interaction effects are negligible. It is interesting to note that the RDG-FA theory predicts the shape of the phase function with very good accuracy for all cases considered, as long as the primary particle size of the aggregate is small (i.e., $x_p < 0.1$). In all cases the deviation between IEFS and RDG-FA theories is below 20%.

In summary, the results presented for cluster–cluster fractal-like aggregates are very encouraging, suggesting that the RDG-FA theory is a good approximation for a large range of primary particle sizes and refractive indices. In particular, and apart from a small region in the upper limits of the domain covered, namely x_p and $|m-1|$ close to 0.1 and 4, respectively, deviations between RDG-FA

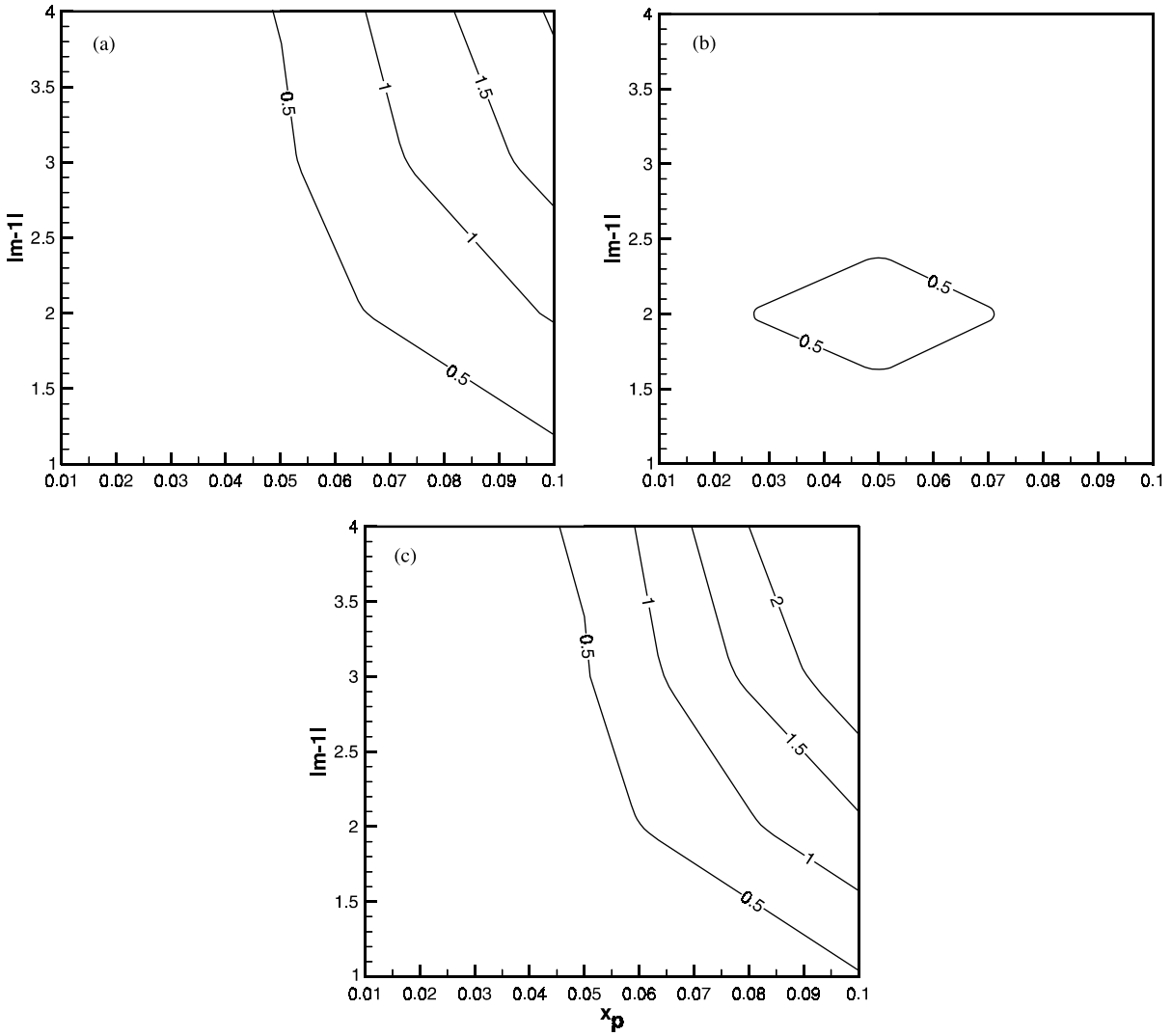

Fig. 3. Contours of the relative error of the phase function calculated using the IEFS theory: (a) $\Theta = 0^{\circ}$; (b) $\Theta = 90^{\circ}$; (c) $\Theta = 180^{\circ}$.

and IEFS predictions are always lower than 30%. Therefore, the RDF-FA theory may be used with due caution to investigate the general impact of aggregation on the optical and radiative properties of soot in the infrared region of the spectrum.

4. Effect of aggregation on the scattering properties of soot

It is well known that scattering is negligible compared with absorption for primary soot particles. This section examines whether this is still true or not for soot agglomerates. Fig. 7 shows the ratio

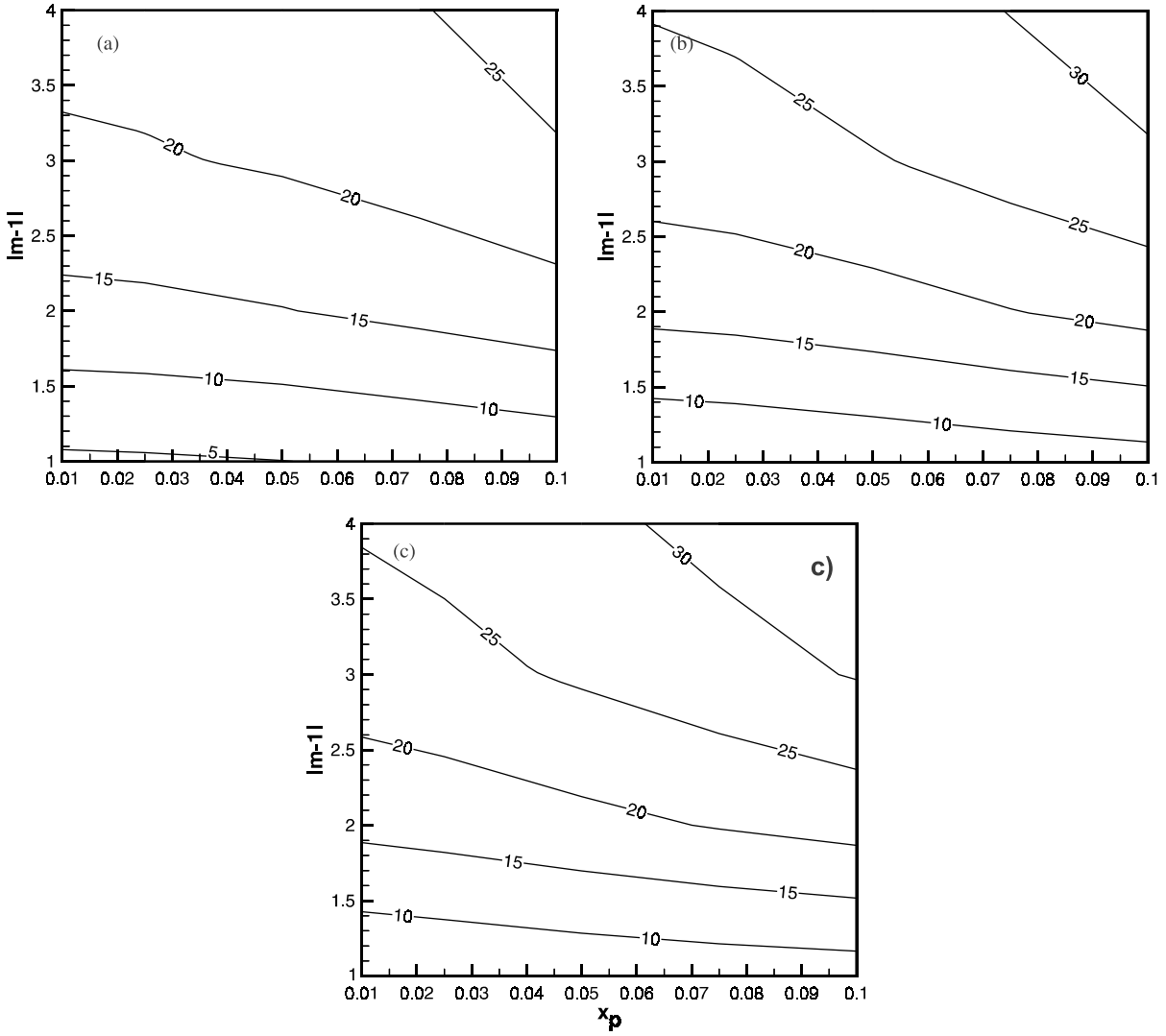

Fig. 4. Percent deviation contours of the RDG-FA predictions from the IEFS results for the absorption cross section of soot aggregates: (a) $N = 16$; (b) $N = 64$; (c) $N = 256$.

of the total scattering cross section to the absorption cross section for different values of the refractive index. It is observed that, for a given complex refractive index, the ratio C_s^a/C_a^a increases with N for a fixed x_p, and increases with x_p for a fixed N. For an aggregate with given x_p, the ratio increases with $|m-1|$, i.e., with the wavelength. The absorption cross sections are consistently superior to scattering cross sections throughout the range of properties under investigation. However, for large values of m, N and x_p, absorption and total scattering cross sections are of the same magnitude, i.e. $C_s^a/C_a^a > 0.1$. For example, scattering may become relevant when compared with absorption for aggregates with $N > 200$, $x_p \approx 0.1$ and $|m-1| > 2$, because of the relatively high scattering cross section combined with a phase function dominated by forward scattering.

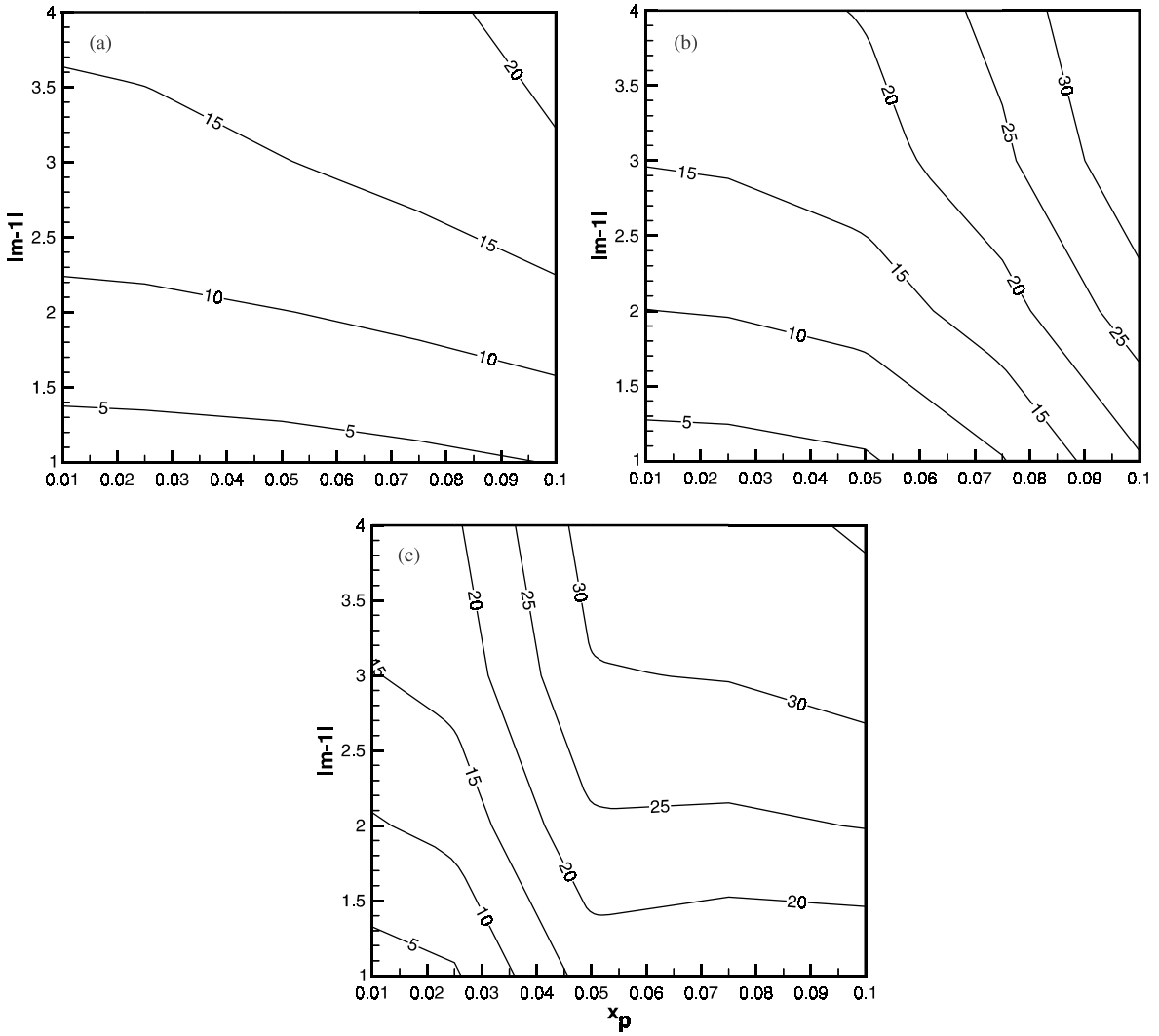

Fig. 5. Percent deviation contours of the RDG-FA predictions from the IEFS results for the scattering cross section of soot aggregates: (a) $N = 16$; (b) $N = 64$; (c) $N = 256$.

Eq. (6) shows that scattering is directly proportional to N^2 as long as the aggregates are small, i.e., dominated by the small angle (Guinier) regime, and therefore the impact of aggregation grows linearly with N. However, as the aggregate size increases, the power-law regime becomes important, continuously reducing the effect of aggregation on the total scattering cross section. This trend has been discussed in the past [8], and can be observed in Fig. 8. Apart form a small region where large N and x_p are combined, the Guinier regime appears to be dominant throughout the scattering angles. Therefore, it can be concluded that scattering is strongly affected by aggregation, i.e. the ratio C_s^a/NC_s^p is proportional to N. Nevertheless, the region where this effect becomes less important (large N and x_p) coincides with the one where scattering becomes more important when compared

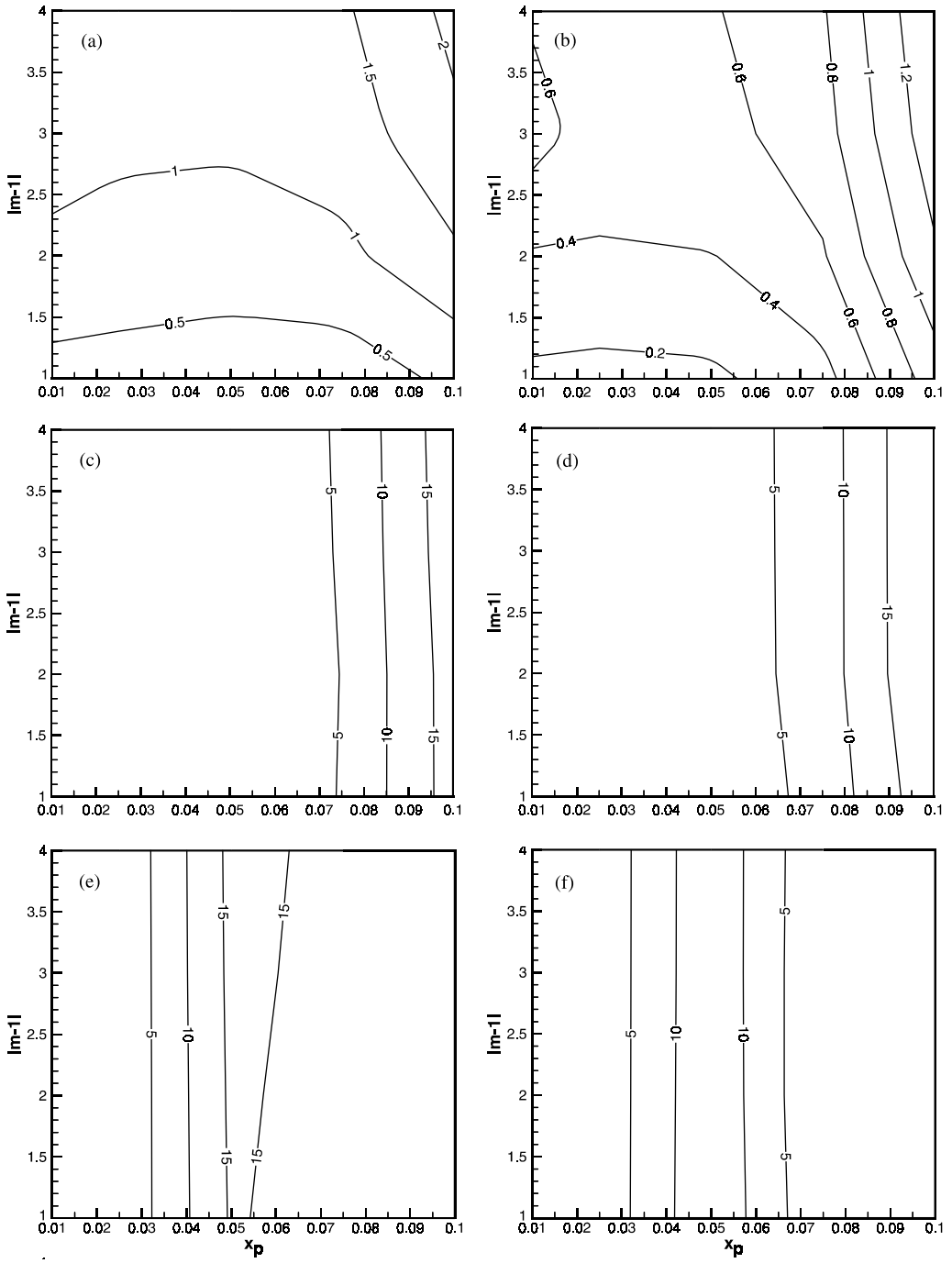

Fig. 6. Percent deviation contours of the RDG-FA predictions from the IEFS results for the phase function of soot aggregates: (a) $N = 16$, $\Theta = 0^{\circ}$; (b) $N = 16$, $\Theta = 90^{\circ}$; (c) $N = 64$, $\Theta = 0^{\circ}$; (d) $N = 64$, $\Theta = 90^{\circ}$; (e) $N = 256$, $\Theta = 0^{\circ}$; (f) $N = 256$, $\Theta = 90^{\circ}$.

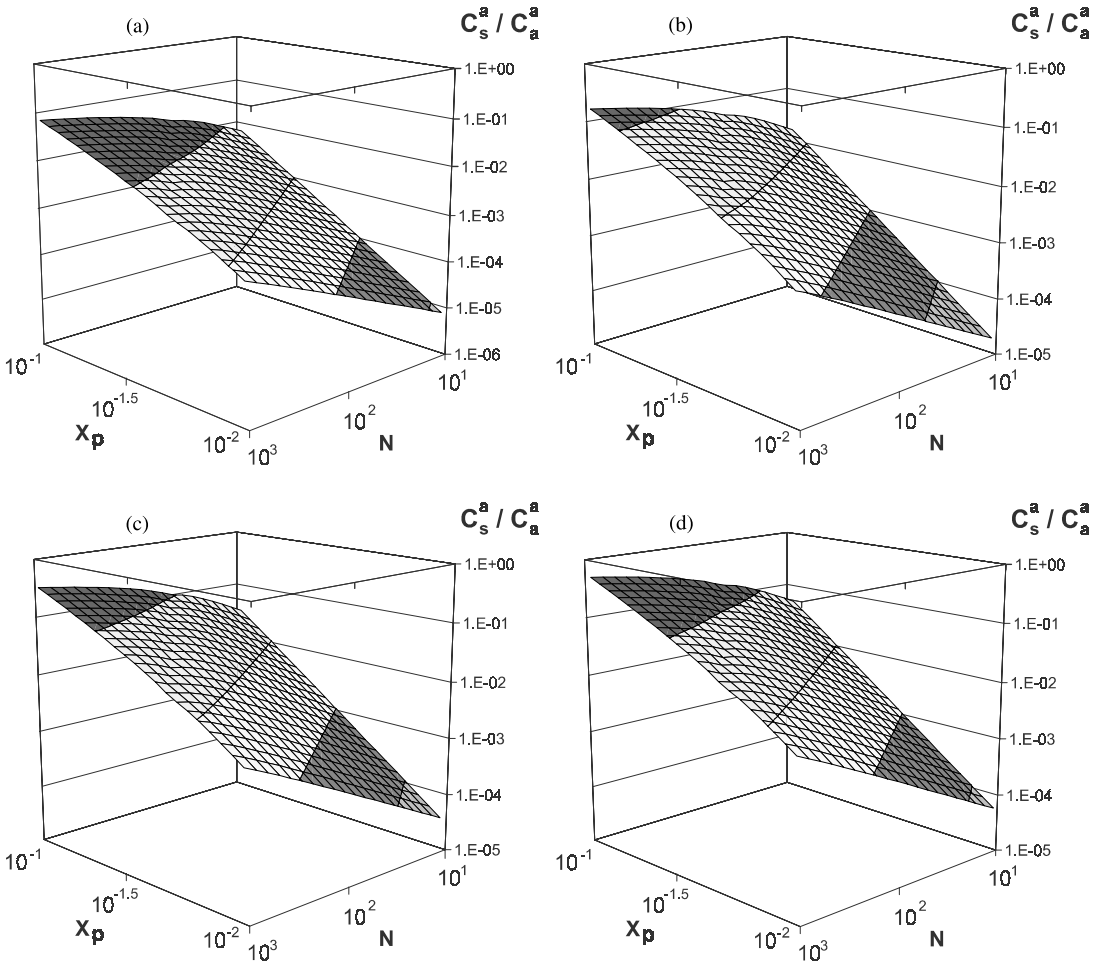

Fig. 7. Surface plot of C_s^a/C_a^a showing the effect of scattering compared with absorption: (a) $|m-1|=1$; (b) $|m-1|=2$; (c) $|m-1|=3$; (d) $|m-1|=4$.

with absorption. This suggests that in most practical situations the impact of aggregation will not be severe.

Fig. 9 shows the phase function of a population of aggregates with $N=256$, $x_p=0.1$ and $|m-1|=1$ calculated using the RDG-FA theory. The predictions obtained using the Mie theory for a sphere with the same volume and a single Rayleigh scatterer are also plotted. It is worth to point out that none of these methods (RDG-FA, Mie theory for a sphere with the same volume and single Rayleigh scatterer) reflect reality, and so the results obtained must be regarded with caution. Nevertheless, they have been used here since more accurate theories are not currently available, apart from the IEFS theory, which has been shown to yield results relatively close to the RDG-FA theory for the range of parameters under consideration. Fig. 9 shows that neither Mie equivalent volume spheres nor Rayleigh scatterers predict the highly forward phase functions that fractal-like aggregates such as soot exhibit. In fact, the forward to backward scattering ratio $\Phi(0^\circ)/\Phi(180^\circ)$ predicted by RDG-FA

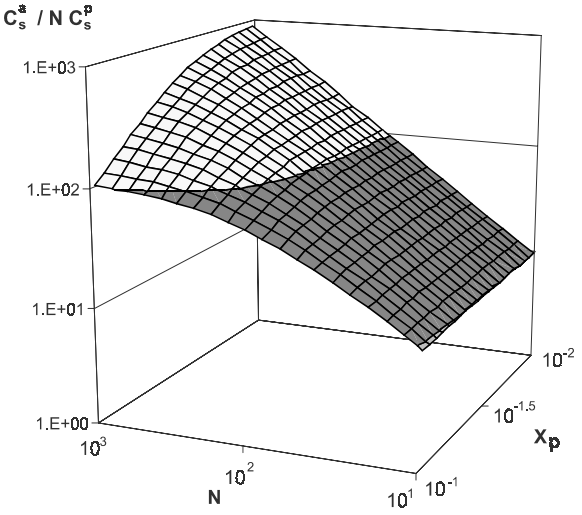

Fig. 8. Effect of aggregation on the total scattering cross section.

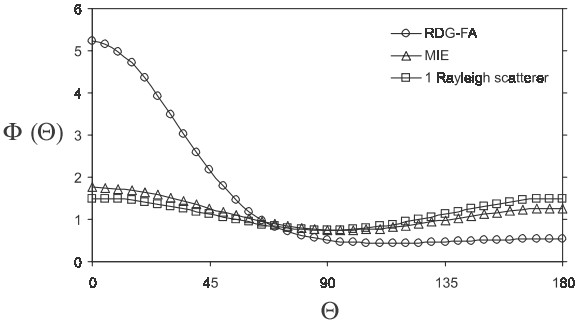

Fig. 9. Phase function of a population of aggregates with $N = 256$, $x_p = 0.1$ and $|m - 1| = 1$ calculated using the RDG-FA theory, the Mie theory for an equivalent volume sphere and the Rayleigh theory for a single particle.

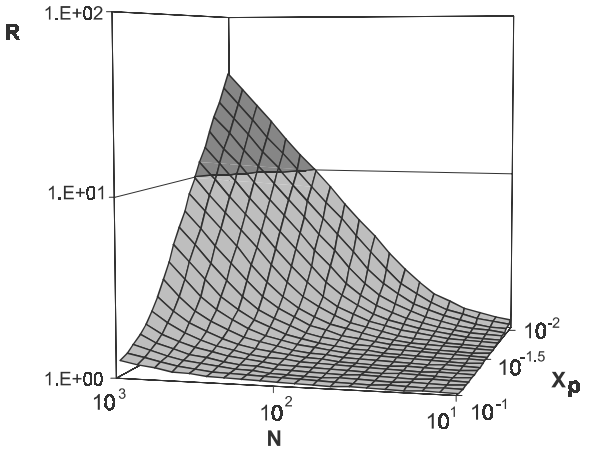

Fig. 10. Influence of aggregation on the shape of the phase function. R is defined as $[\Phi(0^\circ)/\Phi(180^\circ)]_a/[\Phi(0^\circ)/\Phi(180^\circ)]_p$.

is about 10, while the ratio computed using either Mie or Rayleigh theories is of the order of 1. Additional calculations were carried out for values of $|m - 1|$ up to 4 using the appropriate wavelengths. It was found that the strong forward peak observed in Fig. 9 for the RDG-FA theory becomes substantial small as m increases, and the difference between the results predicted by the different methods decreases, becoming negligible for $|m - 1| = 4$.

The importance of aggregation on the shape of the phase function, namely on the forward scattering peak, is illustrated in Fig. 10, which shows a 3D surface map of R, defined as $[\Phi(0^\circ)/\Phi(180^\circ)]_a/$

$[\Phi(0^\circ)/\Phi(180^\circ)]_p$, the subscripts a and p standing for an aggregate and a primary particle, respectively. The results show that R is large, i.e., aggregation has a strong impact on the shape of the phase function, if both N and x_p are large.

5. Influence of soot aggregation on radiative transfer calculations

The influence of soot aggregation on radiative transfer calculations is investigated in this section. Radiative transfer between two parallel infinite black walls at 300 K is considered. The medium between the walls is at a temperature of 2000 K, and contains a uniform distribution of soot, but no participating gases. The distance between the plates is taken as $L = 1$ m. It is assumed that soot forms agglomerates with $N = 256$ and $d_p = 50$ nm. The soot volumetric fraction, f_v, varies in the range 10^{-6}–10^{-5}. The data for the refractive index of acetylene soot as a function of wavelength reported in [33] is used in the present calculations. The radiative properties of soot are calculated according to the RDG-FA theory.

The problem described above has an exact solution if there is no scattering and the absorption coefficient of the medium is prescribed (see, e.g., [15]). However, there is no analytical solution if scattering is taken into account. Since our main goal is to investigate the influence of scattering in the presence of soot aggregates on radiative heat transfer, a radiation model was used both with and without scattering. The calculations were performed using the discrete ordinates method [34], the step discretization scheme [35], a uniform grid with 101 control volumes, and an angular discretization with 10 polar and azimuthal equally spaced divisions per octant, yielding 100 discrete ordinates per octant. The quadrature weights are taken as the areas of the unit sphere that subtend the solid angles resulting from the angular discretization, like in the finite volume method [36]. This allows a much finer angular discretization than if the popular S_N quadratures were used, since the order of these quadratures is limited by the appearance of negative weights. It was found that the S_{16} quadrature does not accurately integrate the phase functions with a strong forward peak that occur for low values of $|m - 1|$, contrary to the selected angular discretization. The dependence of the radiative properties on the wavelength was accounted for by dividing the spectrum from 0 to 100 μm into 40 non-uniform intervals, and integrating the radiative transfer equation over each interval [37].

Fig. 11 shows the predicted radiative heat source, $\nabla \cdot \mathbf{q}$, where $\mathbf{q}$ is the heat flux vector. The profile is flat in the central region of the domain and increases sharply towards the walls in their vicinity. The radiative source at the center of the domain decreases with the increase of soot volumetric fraction because the optical thickness of the medium becomes so large that the emitted radiation is rapidly absorbed, and radiation loss is only significant in the neighborhood of the colder walls. However, the heat flux incident on the walls increases with the increase of soot volumetric fraction, as expected.

The radiative source profiles plotted in Fig. 11 were computed without scattering, but those calculated with scattering are almost indistinguishable from them. This means that scattering may be neglected in heat transfer calculations even for the high soot concentrations and large aggregates under consideration. To give a better insight on the reason why the role of soot scattering is marginal, the predicted spectral radiative heat source, $\nabla \cdot \mathbf{q}_\lambda$, at the center of the domain ($x = L/2$) is shown in Fig. 12. Similar conclusions would be drawn if other points were selected, but the influence of scattering would be even lower. Fig. 12 also shows the relative difference between calculations of

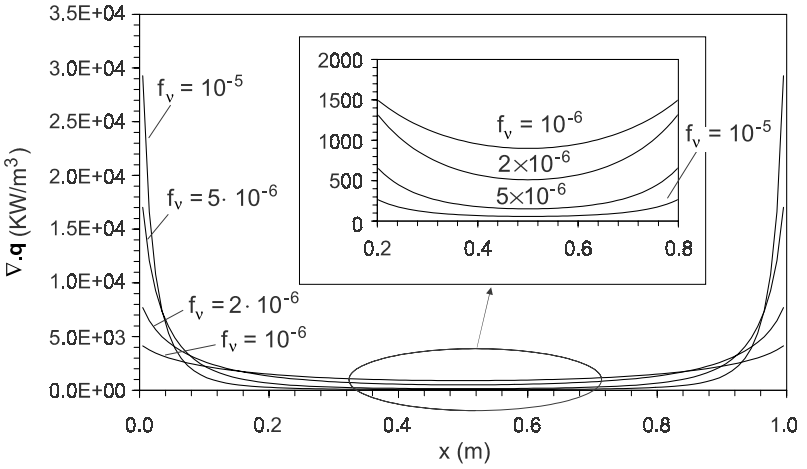

Fig. 11. Predicted radiative heat source between two parallel infinite black walls as a function of soot volumetric fraction.

the spectral radiative source neglecting scattering (subscript ns) and those accounting for scattering (subscript s), denoted by ε:

$$\varepsilon = |(\nabla \cdot \mathbf{q}_\lambda)_{\mathrm{ns}} - (\nabla \cdot \mathbf{q}_\lambda)_{\mathrm{s}}|/(\nabla \cdot \mathbf{q}_\lambda)_{\mathrm{ns}}. \tag{14}$$

The calculations performed without scattering were compared with the exact solution [15], and it was found that the error is of the order of 0.1%.

Fig. 12a shows that the spectral radiative source profile exhibits a maximum, which is displaced to longer wavelengths if the soot volumetric fraction increases. The relative difference between the calculations with scattering and those without scattering, ε, may achieve quite high values for short wavelengths, but decreases sharply with the increase of the wavelength. In fact, it was shown above that the phase function has a strong forward peak for $|m-1|=1$, and these values of the refractive index occur for short wavelengths. As the wavelength increases, so does $|m-1|$, and the phase function approaches that of a Rayleigh scatterer. In this situation, absorption is dominant and scattering is negligible. For example, if $f_{\mathrm{v}} = 10^{-6}$, then ε is $> 5\%$ if $\lambda < 1$ μm. However, in the region where $\lambda < 1$ μm, the contribution of $\nabla \cdot \mathbf{q}_\lambda$ to $\nabla \cdot \mathbf{q}$ is very small, and therefore the influence of scattering is marginal. Although the evaluation of the RDG-FA theory presented above has been restricted to x_{p} up to 0.1, which corresponds approximately to $\lambda > 1.5$ μm, previous studies have shown that the theory is also reliable for larger values of x_{p}, i.e., shorter wavelengths, provided that $|m-1|$ does not exceed the unity [8,9]. If $f_{\mathrm{v}} = 2 \times 10^{-6}$, then ε is $> 5\%$ if $\lambda < 2$ μm, and exceeds 10% for $\lambda < 1.3$ μm. However, the contribution of these short wavelengths to the total radiative source is small, as illustrated in Fig. 12a, and therefore the influence of scattering to the total radiative source is again very small. The range of wavelengths where scattering is important increases with the increase of f_{v}, but remains confined to a region of the spectrum that has a little contribution to the total radiative source. Even for f_{v} as large as 10^{-5} the influence of scattering on the total radiative source is negligible.

The influence of the distance between the walls is examined in Fig. 13 for $f_{\mathrm{v}} = 10^{-5}$. It can be seen that L has a very important influence on the value of the radiative heat source, but the influence

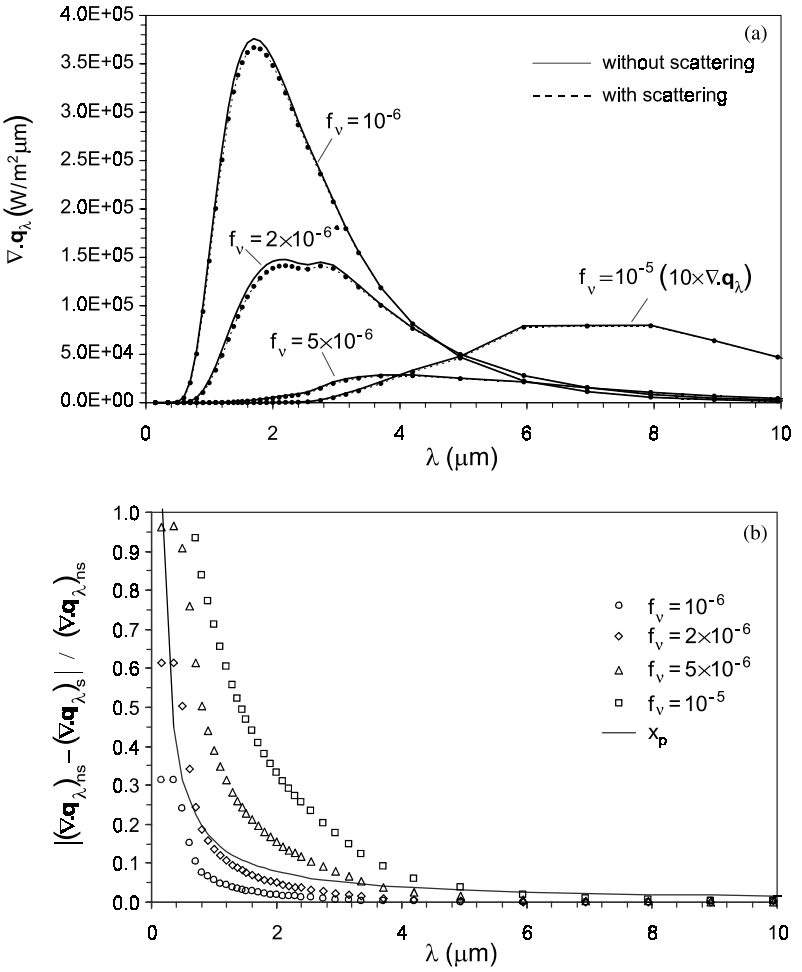

Fig. 12. Predicted spectral radiative heat source at a point equidistant from two parallel infinite black walls as a function of soot volumetric fraction. (a) Predicted spectral profiles computed with and without scattering. (b) Relative difference between the calculations with scattering and the calculations without scattering.

of scattering is again negligible. In fact, if the distance between the walls increases, so does the range of wavelengths where scattering is relevant, but the region where the spectral radiative heat source is largest shifts to longer wavelengths.

The radiative heat source at $x = L/2$ and the incident heat flux on the walls are given in Tables 1 and 2, respectively, for calculations with and without scattering, and for the range of f_v and L reported above. The radiative heat source does not differ by $> 3\%$ between the two sets of calculations, except in the case of $f_v = 10^{-5}$ and $L = 10$ m where scattering yields a radiative heat source that is about 6% lower than that calculated without scattering. The incident heat fluxes are even closer for the two sets of calculations, differing by no more than 0.62%.

Additional calculations were performed for a temperature of the medium equal to 1500 K, and the results are very similar to those reported above. Finally, the calculations were repeated for aggregates

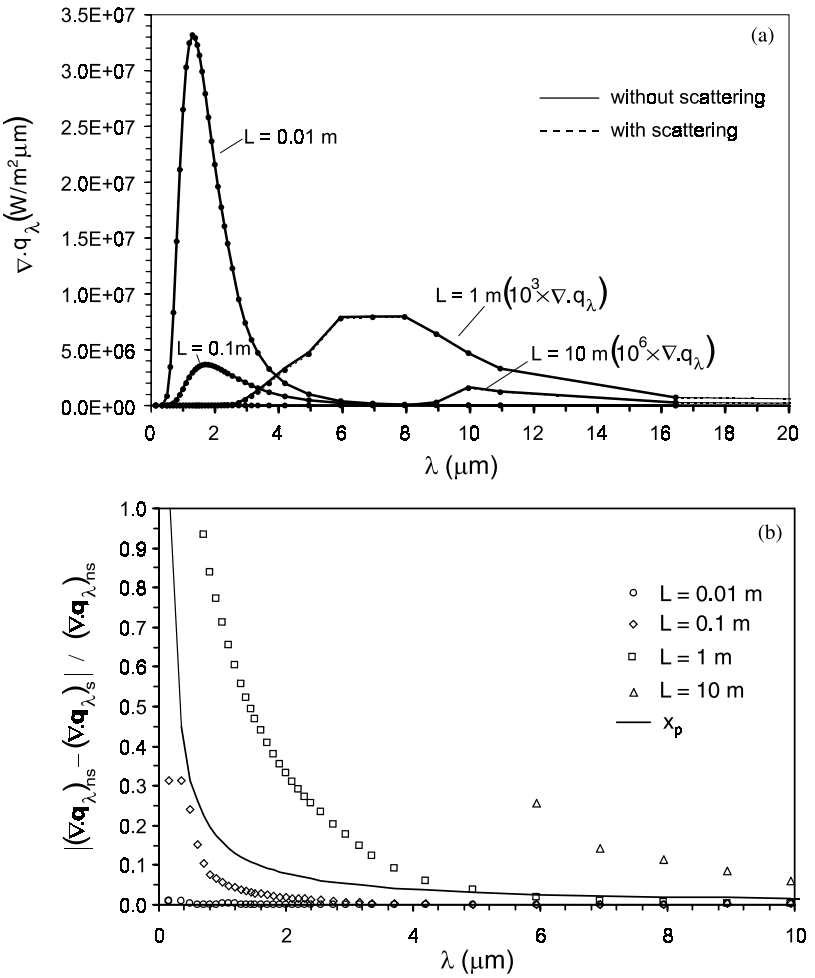

Fig. 13. Predicted spectral radiative heat source at a point equidistant from two parallel infinite black walls as a function of the distance between the walls. (a) Predicted spectral profiles computed with and without scattering. (b) Relative difference between the calculations with scattering and the calculations without scattering.

Table 1
Radiative heat source at $x = L/2$ for $N = 256$

f_v	L (m)	$(\nabla \cdot \mathbf{q})_{ns}$ (kW/m^3)	$(\nabla \cdot \mathbf{q})_s$ (kW/m^3)
10^{-6}	1.00	900.00	884.07
2×10^{-6}	1.00	511.81	497.15
5×10^{-6}	1.00	152.70	148.86
10^{-5}	1.00	59.08	58.24
10^{-5}	0.01	5.55×10^{4}	5.56×10^{4}
10^{-5}	0.10	9.00×10^{3}	8.84×10^{3}
10^{-5}	10.00	7.83×10^{-3}	7.36×10^{-3}

Table 2
Incident radiative heat fluxes at the wall for $N = 256$

f_v	L (m)	$(\mathbf{q}_w)_{ns}$ (kW/m^2)	$(\mathbf{q}_w)_s$ (kW/m^2)
10^{-6}	1.00	811.1	807.5
2×10^{-6}	1.00	870.9	865.6
5×10^{-6}	1.00	891.6	892.3
10^{-5}	1.00	904.6	899.2
10^{-5}	0.01	289.4	289.8
10^{-5}	0.10	811.1	807.5
10^{-5}	10.00	907.2	904.9

with $N=1024$. Although the evaluation of the RDG-FA theory has not been extended to such a high value of N, and the accuracy may be lower, the results obtained show that the incident heat fluxes and radiative heat sources are only slightly different from those calculated for $N=256$. For example, for $f_v = 10^{-5}$ and $L = 1$ m, the incident heat flux is 898.6 kW/m^2 and the radiative heat source at $x = L/2$ is 57.64 kW/m^3 for $N = 1024$, compared to 899.2 kW/m^2 and 58.24 kW/m^3, respectively, for $N = 256$. The maximum difference between the two sets of calculations does not exceed 0.7% for the incident heat flux and 3.5% for the radiative heat source for the range of parameters under consideration, except for $f_v = 10^{-5}$ and $L = 10$ m where the difference between the radiative heat sources increases to 11.7%. This suggests that scattering remains negligible for such large soot aggregates.

6. Conclusions

The effect of aggregation on soot optical properties was investigated emphasizing the infrared region of the spectrum. The numerical study was performed quantitatively using the RDG-FA theory. An evaluation of the accuracy of this theory was performed by means of comparison of predicted phase functions, scattering and absorption coefficients with the results of the more accurate IEFS theory, in order to investigate the applicability of the RDG-FA theory to a wide range of aggregate sizes and wavelengths. Following the successful evaluation, the RDG-FA method was used to investigate the effects of aggregation on soot optical cross-sections and phase function. The results of this study allow us to distinguish two main situations of interest. If N and x_p are both low (small aggregates formed with small primary particles) the results show that the scattering coefficient is negligible compared to the absorption coefficient. Within this range, scattering and aggregation of primary particles can be ignored. Thus, the Rayleigh approximation can be used leading to isotropic scattering. On the other hand, if both N and x_p are large, aggregation starts to become important, contributing to an increase in the scattering cross sections, which reach values of the same order of magnitude of the absorption cross sections. In addition, the phase function becomes highly peaked in the forward direction. Therefore, the Rayleigh and equivalent volume Mie sphere approximations appear to be no longer applicable, and the RDG-FA method emerges as a good compromise between accuracy and simplicity of application. However, calculations performed for radiative transfer between two infinite, parallel, black walls with a medium constituted by a transparent gas and soot have shown that scattering from soot may be neglected even for large soot aggregates and high soot concentration. In fact, the spectral radiative heat source is small in the region of the spectrum where scattering is significant, no matter the distance between the walls. Therefore, the spectral region where scattering is important has a marginal contribution to the total radiative source and incident heat fluxes.

Acknowledgements

The financial support of ICCTI (Instituto de Cooperação Científica e Tecnológica Internacional) and French embassy in Lisbon within the framework of project 304-B4 is acknowledged. Part of the present research work was funded by FCT (Fundação para a Ciência e a Tecnologia) through project PRAXIS EME/12035/1998.

References

[1] Tien CL, Lee SC. Flame radiation. Prog Energy Combust Sci 1982;8:41–59.
[2] Viskanta R, Mengüç MP. Radiation heat transfer in combustion systems. Prog Energy Combust Sci 1987;13:97–160.
[3] Siegel R, Howell JR. Thermal radiation heat transfer. New York: Hemisphere, 1992.
[4] Megaridis CM, Dobbins RA. Morphological description of flame-generated materials. Combust Sci Tech 1990;77:95–109.
[5] Köylü ÜÖ, Faeth GM. Structure of overfire soot in buoyant turbulent diffusion flames at long residence times. Combust Flame 1992;89:140–56.
[6] Charalampopoulos TT, Chang H. Effects of soot agglomeration on radiative transfer. JQSRT 1991;46:125–34.
[7] Ku JC, Shim K-H. Optical diagnostics and radiative properties of simulated soot agglomerates. J Heat Transfer 1992;113:953–8.
[8] Farias TL, Carvalho MG, Köylü ÜÖ, Faeth GM. Computational evaluation of approximate Rayleigh–Debye–Gans/fractal-aggregate theory for the absorption and scattering properties of soot. J Heat Transfer 1995;117:152–9.
[9] Farias TL, Carvalho MG, Köylü ÜÖ. The range of validity of the Rayleigh–Debye–Gans/fractal-aggregate theory for computing optical properties like fractal aggregates. Appl Opt 1996;35:6560–7.
[10] Sorensen CM, Cai J, Lu N. Test of static structure factors for describing light scattering from fractal soot aggregates. Langmuir 1992;8:2064–9.
[11] Manickavasagam S, Mengüç MP. Scattering matrix elements of fractal-like soot agglomerates. Appl Opt 1997;36:1337–51.
[12] Köylü ÜÖ, Faeth GM. Optical properties of soot in buoyant turbulent diffusion flames at long residence times. J Heat Transfer 1994;116:152–9.
[13] Farias TL, Carvalho MG, Köylü ÜÖ. Radiative heat transfer in soot combustion systems with aggregation. Int J Heat Mass Transfer 1998;41:2581–7.
[14] Lou W, Charalampopoulos TT. On the electromagnetic scattering and absorption of agglomerated small spherical particles. J Phys D: Appl Phys 1994;27:2258–70.
[15] Modest MF. Radiative heat transfer. New York: Mc-Graw Hill, 1993.
[16] Freltoft T, Kjems JK, Sinha SK. Power-law correlations and finite size effects in silica particle aggregates studied by small-angle neutron scattering. Phys Rev B 1986;33:269–75.
[17] Julien R, Botet R. Aggregation and fractal aggregates. Singapore: World Scientific Publishing Co., 1987.
[18] Martin JE, Hurd AJ. Scattering from fractals. J Appl Cryst 1987;20:61–78.
[19] Dobbins RA, Megaridis CM. Absorption and scattering of light by polydisperse aggregates. Appl Opt 1991;30:4747–54.
[20] Köylü ÜÖ, Faeth GM. Radiative properties of flame-generated soot. J Heat Transfer 1993;115:409–17.
[21] Bohren CF, Huffman DR. Absorption and scattering of light by small particles. New York: Wiley, 1983.
[22] Kerker M. The scattering of light and other electromagnetic radiation. New York: Academic Press, 1969.
[23] Mackowski DW. Electrostatics analysis of radiative absorption by sphere clusters in the Rayleigh limit: application to soot particles. Appl Opt 1995;34:3535–45.
[24] Brasil AM, Farias TL, Carvalho MG. A recipe for image characterization of fractal-like aggregates. J Aerosol Sci 1999;33:1379–89.
[25] Brasil AM, Farias TL, Carvalho MG. Evaluation of the fractal properties of cluster–cluster aggregates. Aerosol Sci Technol 2000;33:440–54.
[26] Wu M, Friedlander SK. Note on the power-law equation for fractal-like aerosol agglomerates. J Coll Int Sci 1993;159:246–8.
[27] Köylü ÜÖ, Faeth GM, Farias TL, Carvalho MG. Fractal and projected structure properties of soot agglomerates. Combust Flame 1995;110:621–33.
[28] Cai J, Lu N, Sorensen CM. Analysis of fractal cluster morphology parameters: structural coefficient and density autocorrelation function cutoff. J Coll Int Sci 1995;171:470–3.
[29] Samson RJ, Mulholland GW, Gentry JW. Structural analysis of soot aggregates. Langmuir 1987;3:272–81.
[30] Oh C, Sorensen CM. The effect of overlap between monomers on the determination of fractal cluster morphology. J Coll Int Sci 1997;193:17–25.

[31] Ku JC, Shim KH. A comparison of solutions for light scattering and absorption by agglomerated or arbitrarily-shaped particles. JQSRT 1992;47:201–20.
[32] Purcell EM, Pennypacker CR. Scattering and absorption of light by nonspherical dielectric grains. Astrophys J 1973;186:705–14.
[33] Dalzell WH, Sarofim AF. Optical constants of soot and their application to heat flux calculations. J Heat Transfer 1969;91:100–4.
[34] Chandrasekhar S. Radiative transfer. New York: Dover Publications, Inc., 1960.
[35] Chai JC, Lee HS, Patankar SV. Evaluation of spatial differencing practices for the discrete ordinates method. J Thermophys Heat Transfer 1994;8:140–4.
[36] Raithby GD, Chui EH. A finite-volume method for predicting a radiant heat transfer in enclosures with participating media. J Heat Transfer 1990;112:415–23.
[37] Fiveland WA, Jamaluddin AS. Three-dimensional spectral radiative heat transfer solutions by the discrete-ordinates method. J Thermophys Heat Transfer 1991;5:335–9.